Polymorphism, Mesomorphism, and Metastability of Monoelaidin in Excess Water

Hesson Chung and Martin Caffrey
Department of Chemistry, The Ohio State University, Columbus, Ohio 43210 USA

ABSTRACT The polymorphic and metastable phase behavior of monoelaidin dry and in excess water was studied by using high-sensitivity differential scanning calorimetry and time-resolved x-ray diffraction in the temperature range of 4°C to 60°C. To overcome problems associated with a pronounced thermal history-dependent phase behavior, simultaneous calorimetry and time-resolved x-ray diffraction measurements were performed on individual samples.

Monoelaidin/water samples were prepared at room temperature and stored at 4°C for up to 1 week before measurement. The initial heating scan from 4°C to 60°C showed complex phase behavior with the sample in the lamellar crystalline (L_{c0}) and cubic (Im3m, Q^{229}) phases at low and high temperatures, respectively. The L_{c0} phase transforms to the lamellar liquid crystalline (L_α) phase at 38°C. At 45°C, multiple unresolved lines appeared that coexisted with those from the L_α phase in the low-angle region of the diffraction pattern that have been assigned previously to the so-called X phase (Caffrey, 1987, 1989). With further heating the X phase converts to the Im3m cubic phase. Regardless of previous thermal history, cooling calorimetric scans revealed a single exotherm at 22°C, which was assigned to an L_α + cubic (Im3m, Q^{229})-to-lamellar gel (L_β) phase transition. The response of the sample to a cooling followed by a reheating or isothermal protocol depended on the length of time the sample was incubated at 4°C. A model is proposed that reconciles the complex polymorphic, mesomorphic, and metastability interrelationships observed with this lipid/water system.

Dry monoelaidin exists in the lamellar crystalline (β) phase in the 4°C to 45°C range. The β phase transforms to a second lamellar crystalline polymorph identified as β^* at 45°C that subsequently melts at 57°C. The β phase observed with dry monoelaidin is identical to the L_{c0} phase formed by monoelaidin that was dispersed in excess water and that had not been previously heated.

INTRODUCTION

The monoacylglycerols are important intermediates in lipid metabolism. Although they are not major constituents of most cellular membranes, their capacity to express a wide assortment of liquid crystalline states or mesophases at and close to physiological conditions (Lutton, 1965) suggests that small amounts may have a significant impact on membrane lipid phase behavior and, by extension, membrane function. Monoelaidin, the focus of the current study, is representative of this group of lipids and is of interest because of the rich mesomorphism it exhibits when dispersed in water. Several of these mesophases are metastable, a feature that may enable certain organisms to survive extreme fluctuations in environmental conditions (Mariani et al., 1988).

Monoelaidin incorporates an ester-linked 18-carbon-atom-long fatty acid with a *trans* double bond at the C9 position of the acyl chain. In addition to its rich mesomorphic behavior when hydrated, monoelaidin exhibits polymorphism in the dry state (Bailey, 1950; Maruyama et al., 1982). The latter refers to the existence of more than one crystalline modification and is frequently encountered in dry and hydrated lipids (Garti and Sato, 1988) and surfactants (Kekicheff, 1989). The polymorphic behavior of dry glycerides has been studied extensively (Garti and Sato, 1988; Small, 1986). The temperature-composition (T-C) phase diagram of monoelaidin in water constructed three decades ago includes the lamellar crystalline and L_α phases in the low-temperature/low-hydration region, a cubic phase at elevated temperatures, and high water contents and the fluid isotropic (FI) phase in the high-temperature region (Lutton, 1965). More recently, time-resolved x-ray diffraction (TRXRD) was used to construct phase diagrams for monoelaidin as a function of salt and water concentration (Caffrey, 1985, 1987). Interestingly, salt has the effect of stabilizing the inverted hexagonal (H_{II}) phase, which was not seen in this system in its absence. The effect of hydration on the lamellar structure of monoelaidin has been examined in some detail (McIntosh et al., 1989). In all of these studies, measurements were made at and above room temperature. To the best of our knowledge, the low-temperature polymorphic and mesophase behavior of monoelaidin in the presence of water has not been investigated.

As part of a research program aimed at establishing the relationship between lipid molecular structure and mesophase behavior, we have examined the phase properties of monoelaidin in the 4°C to 60°C range and have found that the lipid can exist in at least three different lamellar crystalline (L_c) polymorphic forms in addition to the lamellar gel phase below room temperature (26°C). The latter is not stable thermodynamically and transforms to an L_c phase upon isothermal incubation at low temperature.

Received for publication 8 May 1995 and in final form 31 July 1995.
Address reprint requests to Dr. Martin Caffrey, Department of Chemistry, Ohio State University, 120 W. 18th Ave., Columbus, OH 43210. Tel.: 614-292-8437; Fax: 614-292-1532; E-mail: caffrey + @osu.edu.
© 1995 by the Biophysical Society
0006-3495/95/11/1951/00 $2.00

To decipher the complex polymorphic and metastable mesophase behavior of monoelaidin in excess water, we have used calorimetry and TRXRD. High-sensitivity differential scanning calorimetry (HSDSC) provided the thermodynamic information. Additionally, we have employed simultaneous calorimetry and TRXRD (SCALTRD) to correlate unambiguously thermal events and structural changes in a manner that eliminates the complexities associated with a polymorphic and mesomorphic behavior that is strongly thermal history-dependent. Separate TRXRD measurements have also been performed to facilitate mesophase identification in complex mixtures of phases and for high-resolution structure characterization. Finally, static x-ray diffraction measurements on powder samples at fixed temperatures were used to decipher the structure of the L_{c0} phase.

EXPERIMENTAL PROCEDURES

Materials

Monoelaidin obtained from Nu-Chek-Prep (Elysian, MN) had a purity of ≥99% as judged by thin-layer chromatography on silica gel K5F plates (Alltech Assoc., Deerfield, IL) of >100 μg lipid in three solvent systems (chloroform/methanol/water, 65:25:4 by vol; hexane/toluene/acetic acid, 60:40:1 by vol; chloroform/acetone/acetic acid/methanol, 72.5:25:0.5:2 by vol) and was used without further purification. At room temperature, monoelaidin consists of 90 to 92% 1-monoelaidin and 8 to 10% of 2-monoelaidin (Martin, 1953). All other chemicals used were of reagent grade. Water was purified by using a Milli-Q water purification system (Millipore Corp., Bedford, MA).

X-ray source

The measurements were made in the A1 station at the Cornell High-Energy Synchrotron Source (CHESS). Experiments were carried out by using wiggler-enhanced, monochromatic (1.56 Å, 8.0 keV), focused x-rays as described previously (Caffrey, 1985, 1987). X-ray wavelength was determined by using a lead nitrate standard and a carefully measured sample-to-film distance. The machine was operating at 5.26 GeV and 80 mA total of electron beam current in the seven-bunch mode and with the six-pole wiggler at half-power. The incident x-ray beam was defined by using either a 0.3-mm- or a 0.5-mm-diameter collimator (Charles Supper Co., Natick, MA) for TRXRD and SCALTRD measurements, respectively. Sample-to-detector distance varied from 11 cm to 40 cm.

Calorimetry

HSDSC was performed on monoelaidin/water samples before the SCALTRD measurements to establish the effect of thermal history on phase behavior and to establish a protocol for the subsequent SCALTRD. Measurements were made with a Microcal MC2 differential scanning calorimeter (DSC) (Microcal, Northampton, MA) operated at a heating scan rate of 50 ± 5°C/h.

Homogeneous samples were prepared by using a home-built lipid mixing device consisting of two 500-μl syringes (Hamilton Co., Reno, NV). Syringes were connected via a coupler that incorporates 6-mm-long, narrow (standard 22-gauge) stainless steel tubing. Approximately 10 mg of lipid was added to one of the syringes as a dry powder and 15 μl of water to the other. The system was flushed with either argon or nitrogen, and the plungers were inserted into the syringe barrels. After adjusting the plungers to expel as much gas as possible, the two syringes were connected via the coupler. The lipid and water were passaged through the coupler from one syringe to the other by working the plungers back and forth at least 500 times at room temperature. Subsequently, the mixture was transferred completely to one of the syringes, and the second syringe and the coupler were disconnected. A 6-inch-long standard 22-gauge needle was attached to the lipid loaded syringe, and the sample was injected into the calorimeter cell. The weight of the sample in the cell was determined by recording the weight (Sartorius MicroM500P, Westbury, NY) of the transfer needle and the syringe before and after sample transfer and by assuming that the sample was homogeneous at the time of transfer. Following this procedure, the sample weight has an associated error of ~10%. Additional water was added directly to the sample cell as above to bring the total sample volume to 1 ml. The reference cell contained 1 ml water. After the cells were loaded, both the sample and the reference cells were flushed with nitrogen in preparation for the calorimetric measurements. Scans were made in the presence of nitrogen, the pressure of which was maintained slightly higher than atmospheric pressure. Between the heating scans, the calorimeter was cooled passively by circulating water at ~0°C through the system using a circulating water bath (Neslab RTE-219, Neslab, Newington, NH). Typically, several hours were needed to cool the sample from 50°C to 4°C with the calorimeter operating in a room at ~25°C. It was not possible to record useful cooling thermograms with the MC2 because the cooling scan rate could not be controlled. Transition enthalpies were calibrated by means of a built-in calibration circuit that uses an electrical pulse of known power and are accurate to ±10%. The transition temperatures are reproducible to ±0.5°C.

SCALTRD and a limited number of low-sensitivity calorimetry (LSC) measurements were made with a Mettler FP84 calorimeter (Mettler Co., Hightstown, NJ). With this device, it was possible to record heating, isothermal, and cooling thermograms. Temperatures below room temperature were achieved by supplying the FP84 with temperature-regulated air from a forced-air crystal heating/cooling apparatus (models XR-85-1A-0 and AD-80XA, FTS Systems, Stone Ridge, NY). Throughout these experiments, a temperature scan rate of 5°C/min was used. The LSC studies using the FP84 were usually performed as a preliminary to the SCALTRD measurements. Scans were made with samples contained in hermetically sealed aluminum crucibles (model 27331, Mettler).

Simultaneous calorimetry and TRXRD

A Mettler FP84 calorimeter was employed for SCALTRD measurements as described previously (Chung and Caffrey, 1992). Thin-walled aluminum crucibles were modified slightly to increase x-ray transmission and were used to contain the lipid samples. This modification increased the x-ray transmittance of the crucible from 4.3×10^{-5}% to 23.1% at 1.55 Å (8.1 keV). The device was mounted with the base of the crucible oriented perpendicular to the synchrotron-derived focused, monochromatic x-ray beam for the SCALTRD data collection. Procedures used to evaluate the effectiveness of crucible sealing have been described (Chung and Caffrey, 1992). Samples consisted of ~10 mg monoelaidin and 25 μl water and were stored for a week at 4°C after preparation at room temperature.

A streak camera incorporating x-ray-sensitive film (DEF5, Eastman Kodak Co., Rochester, NY) was used as a detector for the TRXRD measurements. Film was translated at a rate of 4 mm/min behind a long vertical 3.2-mm-wide slit. Both low- and wide-angle diffraction from the lipid sample was recorded simultaneously on the same film. The calorimeter, streak film, and the calorimetric data collection were under computer (Macintosh IIfx, Apple Computer, Cupertino, CA) control using programs written with LabVIEW (National Instruments Co., Austin, TX) software.

To minimize lipid radiation damage (Caffrey, 1984; Cheng et al., 1993; Chung and Caffrey, 1992), a new portion of the sample was exposed for each SCALTRD measurement. Thus, no one part of the sample was exposed to the x-ray beam for more than 20 min. Experiments to test for radiation damage were carried out before SCALTRD measurements. We assume that the damage is negligible if there is no detectable change in the diffraction pattern during a typical x-ray exposure when other variables, such as temperature, pressure, etc., are held constant. In a monoelaidin/water sample contained in a modified aluminum crucible, a 20-min exposure produced no noticeable change in the diffraction pattern at 38°C.

Temperature-ramping TRXRD

To compensate for the somewhat limited x-ray transmission and temperature and spatial resolution available with SCALTRD, we have performed separate TRXRD measurements. These were made using samples contained in 1-mm-diameter x-ray quartz capillaries (Charles Supper Co.), a 0.3-mm-diameter collimated (Charles Supper Co.) x-ray beam, and a streak camera incorporating a film translating at a speed of 7 mm/min behind a 3.1-mm slit. Sample-to-film distance varied from 16 cm to 40 cm. Temperature ramping was carried out in a home-built Peltier-based temperature regulated sample holder at a heating and cooling rate of ±5°C/min (Briggs and Caffrey, 1994). Temperature control and data acquisition were effected using programs written with LabVIEW software.

During the course of these measurements, no one part of the sample was exposed to the x-ray beam for more than 10 min.

Data analysis

Diffraction patterns recorded on streak film were digitized by using a 1D/2D soft laser scanning densitometer (Biomed Instruments Inc., Fullerton, CA) from which were obtained the intensity versus scattering angle ($I - 2\theta$) scans. The laser beam size was ~40 μm × 2 mm. Frequently, films were scanned repeatedly in the same region and the profiles averaged to increase the signal-to-noise ratio (S/N). On occasion, the streak films were processed manually to retrieve the d-spacing data as a function of temperature.

Static x-ray diffraction

Static x-ray diffraction measurements were performed to compare the phase behavior of powdered monoelaidin samples, dry and in excess water. Samples were contained in 1-mm-diameter x-ray quartz capillaries (Charles Supper Co.), and a 0.3-mm-diameter collimator (Charles Supper Co.) was used. Diffraction patterns were recorded on 8 in × 10 in image plates (prototype storage phosphor, Eastman Kodak Co.) in the A1 station at CHESS. The sample-to-detector distance was 40 cm, and exposure times varied from 30 s to 1 min. To minimize radiation damage and to improve the powder character of the diffraction pattern, the samples were translated continuously at a distance of 2 to 4 mm in the x-ray beam back and forth along the length of the sample. Diffraction patterns were digitized by scanning the plates with the in-house scanner at CHESS. The data were retrieved by using a program written in FORTRAN using a VAX computer.

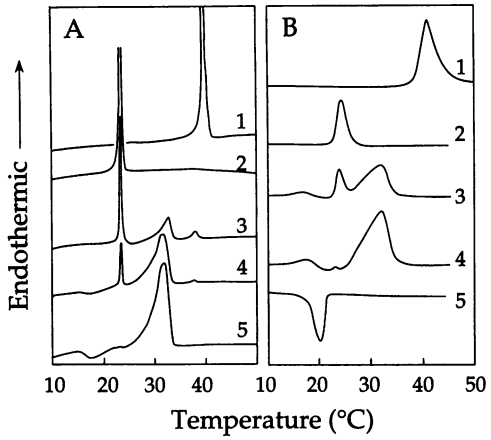

FIGURE 1 Heating and cooling calorimetric thermograms recorded using monoelaidin in excess water with different thermal histories. Data included in (*A*) were collected by means of high-sensitivity differential scanning calorimetry (recorded at a heating scan rate of 0.83°C/min (50.5°C/h)) with the following thermal histories: A1. Dry monoelaidin (2–5 mg) dispersed in excess water (1.0 ml) at 25°C and cooled to 4°C. A2. Sample used in treatment A1 above was cooled to 4°C and immediately heated for use in recording thermogram A2. A3. Sample used in treatment A2 above was cooled to 4°C, incubated at 4°C for 5 min, and then used in heating thermogram A3. A4. Sample used in treatment A3 above was cooled to 4°C, incubated at 4°C for 30 min and then used in recording thermogram A4. A5. Sample used in treatment A4 above was cooled to 4°C, incubated at 4°C for 14 h, and then used in recording heating thermogram A5. Data included in (*B*) were collected using a "lower" sensitivity calorimeter (Mettler FP84) at heating (B1, 2, 3, 4) and cooling (B5) scan rates of 5°C/min (300°C/h) with the following thermal histories: B1. Dry monoelaidin (~10 mg) dispersed in excess water (25 μl) at 25°C was cooled to 4°C. B2. Sample used in treatment B1 was cooled to 4°C and immediately heated for use in recording thermogram B2. B3. Sample used in thermogram B2 was cooled to 4°C, incubated at 4°C for 6 min, and then used in heating thermogram B3. B4. Sample used in thermogram B3 was cooled to 4°C, incubated at 4°C for 15 min, and then used in heating thermogram B4. B5. Sample used in thermogram B2 was used in cooling thermogram B5.

RESULTS

Calorimetry

High-sensitivity differential scanning calorimetry

Heating thermograms of monoelaidin in excess water using HSDSC are shown in Fig. 1 *A*. All scans were obtained using the same sample at a scan rate of 50 ± 5°C/h under identical conditions except for thermal history. The sample contained 2–5 mg of lipid and 1 ml of water. In the initial heating scan, a single sharp endothermic transition was observed at 38°C (the onset temperatures will be used to describe the transition unless otherwise specified) with an enthalpy change (ΔH) of 7.3 ± 0.7 kcal/mol (30.5 ± 3.1 kJ/mol) (Fig. 1 *A1*). During the second and subsequent heating scans performed immediately upon cooling from 47°C to 4°C, this transition was replaced by a sharp endothermic transition at 22.5°C with a ΔH of 6.6 ± 0.7 kcal/mol (27.6 ± 2.8 kJ/mol) (Fig. 1 *A2*). It should be noted that the cooling rate was not regulated in these MC2 measurements and that a cooling scan from 47°C to 4°C lasted several hours. Indeed, up to 1 h was required to adjust the temperature from 10°C to 4°C. After the sample was cooled from 47°C to 4°C, it was incubated at 4°C for 5 min before making the next heating scan. Here, two broad endothermic transitions appeared, one at 12°C and one at 26°C, along with the transition at 22.5°C observed in the original first heating scan with ΔH values of 0.1 ± 0.0, 4.1 ± 0.4, and 4.1 ± 0.4 kcal/mol (0.4 ± 0.1, 17.2 ± 1.7, and 17.2 ± 1.7 kJ/mol), respectively (Fig. 1 *A3*). The transition at 12°C is not obvious at the scale setting used in the thermogram shown in Fig. 1 *A3*, but was seen reproducibly. With longer incubation at 4°C, this transition at 12°C becomes more apparent (Fig. 1, *A4* and *A5*). An endotherm at 38°C was seen for some but not for all samples during second and subsequent heating scans regardless of previous sample history. It is present in the scan shown in Fig. 1, *A3* and *A4*. Upon incubating the sample for 30 min at 4°C, the size of the peak at 22.5°C decreased (ΔH = 1.4 ± 0.1 kcal/mol,

5.9 ± 0.6 kJ/mol), whereas that of peaks at 12°C (ΔH = 0.2 ± 0.0 kcal/mol, 0.8 ± 0.1 kJ/mol) and 26°C (ΔH = 10.8 ± 1.1 kcal/mol, 45.2 ± 4.5 kJ/mol) increased (Fig. 1 *A4*). In the latter thermogram (Fig. 1 *A4*), a broad exotherm at ~16°C (ΔH = −0.2 ± 0.0 kcal/mol, −0.8 kJ/mol) was observed between the transitions at 12°C and 22.5°C. After storing the sample at 4°C for 14 h, the endotherms at 12°C (ΔH = 0.7 ± 0.1 kcal/mol, 2.9 ± 0.3 kJ/mol) and 26°C (ΔH = 15.6 ± 1.6 kcal/mol, 65.3 ± 6.5 kJ/mol) and the exotherm at 16°C (ΔH = −0.7 ± 0.1 kcal/mol, −2.9 ± 0.3 kJ/mol) were observed in the presence of a trace of the 22.5°C transition (Fig. 1 *A5*).

Lower-sensitivity calorimetry

For purposes of comparing the results of the HSDSC (above, Fig. 1 *A*) and LSC measurements, the thermograms obtained with monoelaidin in excess water using the "lower" sensitivity calorimeter (Mettler FP84) at a heating rate of 5°C/min are shown in Fig. 1 *B*. The sample consisted of ~10 mg lipid and 25 μl water. Unlike the high sensitivity calorimeter, it was possible to control the cooling rate on the FP84, which was set to −5°C/min. Generally speaking, the thermograms obtained using LSC and HSDSC were similar, although broader transitions characterized the former. Given the differences in scan rates used (5 vs. 0.83°C/min) this is not unexpected. The initial heating scan with the LSC shows an endothermic transition at 38°C (Fig. 1 *B1*). Subsequent heating scans, performed immediately upon cooling show a single endothermic transition at 23°C (Fig. 1 *B2*). The heating scan after 6 min of incubation at 4°C gave two additional endotherms at 15 and 26°C, along with a diminished peak at 23°C (Fig. 1 *B3*). The LSC heating scans shown in Fig. 1, *B1, B2,* and *B3*, are similar qualitatively to the corresponding HSDSC scans (Fig. 1, *A1, A2,* and *A3*). Quantitative differences are summarized in the following. The transition at ~23°C was barely detectable by LSC when the incubation time at 4°C was increased to 15 min (Fig. 1 *B4*). In contrast, this same transition was quite prominent in the thermogram recorded by HSDSC after a 30-min incubation at 4°C (Fig. 1 *A4*). Indeed, a full 90-min incubation at 4°C was required to eliminate the transition at 23°C under conditions that prevailed for the HSDSC measurements. As noted above, the endothermic transition at 38°C was seen sporadically by HSDSC in second and subsequent heating scans. In contrast, this transition was only present in the initial LSC heating scan. Cooling scans that could only be performed in a controlled manner using the LSC consistently gave a single exothermic transition at 22°C regardless of sample thermal history.

Given the complex nature of the heating thermograms and the relatively simple and repeatable cooling thermal behavior, it was proposed that the low-temperature phase accessed upon cooling was metastable. To test this hypothesis, isothermal calorimetry was performed at 4°C with samples that had been cycled three times between 4°C and 47°C using the lower sensitivity calorimeter (Fig. 2C3). In this measurement, an exothermic event occurred beginning at 6 min (onset time t_o = 6 min) after isothermal conditions were established. Interestingly, t_o varied depending on the particular batch (lot number) of lipid used, as received from a single vender. Batches with lot numbers 244-D4-A and 244-JA27-C gave t_o values of 6 and 13 min, respectively. The samples were equally pure (≥99%) and otherwise exhibited identical thermotropic phase behavior as judged by calorimetry and x-ray diffraction. In this report, results obtained using lipid from lot number 244-D4-A only will be presented.

With the few exceptions noted above, both HSDSC and LSC results were reproducible. This statement is based on measurements repeated ~10 and ~50 times with the high- and low-sensitivity calorimeters, respectively.

Simultaneous calorimetry and TRXRD

From the foregoing, it is apparent that thermal history has a profound influence on the phase behavior of the monoelaidin/water system. To decipher the intricacies of the various polymorphic and mesomorphic transitions, we have performed SCALTRD measurements with the Mettler FP84 calorimeter as described under Experimental Procedures at heating and cooling scan rates of 5°C/min. In this study, the thermal treatment of each sample has been controlled rigorously to facilitate the systematic study of the effect of thermal history on phase behavior. Scheme 1 shows the associated thermal histories imposed. Thus, samples (~10 mg lipid, 25 μl water), contained in hermetically sealed crucibles were prepared at room temperature and immediately cooled (C1, see Scheme 1) for storage at 4°C (Inc1) until SCALTRD measurements were performed. Inc1 lasted about 1 week, at which point synchrotron beam time became available. This 1-week incubation at 4°C (Inc1) did not change the phase behavior of the lipid compared to samples that were heated immediately after cooling to 4°C, as judged by low-sensitivity calorimetry. After Inc1, samples were heated from 4°C to 60°C while SCALTRD measurements were performed (H1). The samples were subsequently cooled to 4°C (C2) and subjected to two thermal cycles between 4°C and 47°C (H2, C3, H3, and C4) to ensure that the lipid was hydrated uniformly. At this point, individual samples were brought through one of the following three treatments to study the effect of low temperature incubation on phase behavior. First, one of the samples was heated immediately, i.e., without any incubation at 4°C (H4-0). The second and third samples were incubated at 4°C for 6 min (Inc2-6) and 15 min (Inc2-15) and subsequently heated (H4-6 and H4-15, respectively) for SCALTRD measurements.

The results of the calorimetry and TRXRD components of the SCALTRD study of monoelaidin in water are shown in Fig. 2. Lattice parameters for each of the phases observed by using SCALTRD during the various thermal treatments are presented in Table 1. Each panel in Fig. 2 includes data

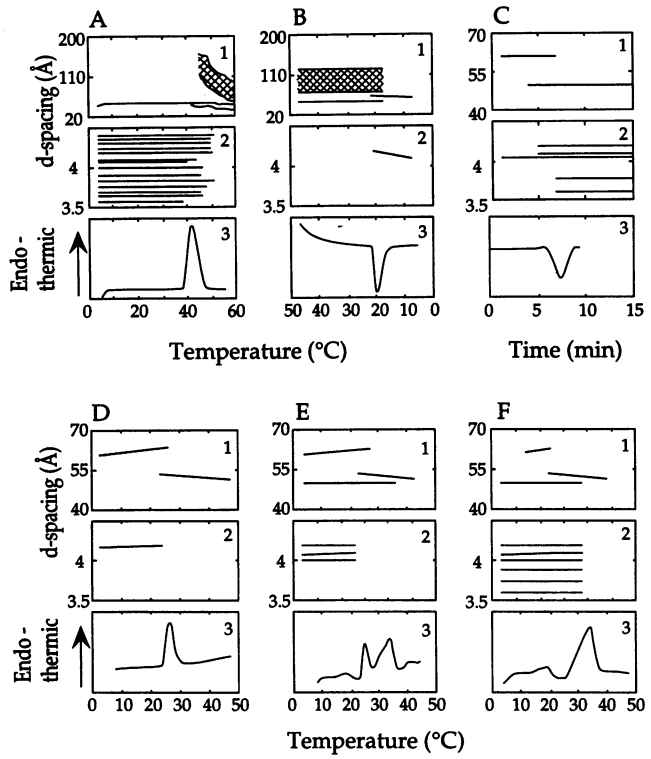

FIGURE 2 Streak film diffraction and calorimetric thermograms recorded for monoelaidin in excess water using time-resolved x-ray diffraction and calorimetric measurements performed simultaneously (*A, B, D–F*) and separately (*C*). Each of the six panels in the figure includes three subpanels labeled 1–3. Subpanels 1 and 2 represent the streak film diffraction data in the low- and wide-angle regions, respectively. Subpanel 3 includes the calorimetric thermograms recorded using the Mettler FP84. Dry monoelaidin (~10 mg) dispersed in excess water (25 μl) at ~25°C and cooled to 4°C was used to collect the SCALTRD data presented in (*A*). The SCALTRD data in (*B*) were collected in the cooling direction after a fully hydrated sample of monoelaidin had been heated to 55°C. (*C*) represents an isothermal study of fully hydrated monoelaidin cooled from 4°C and held for the indicated time interval at 4°C. In this case, calorimetry and TRXRD measurements were made separately. (*D–F*) represent SCALTRD collected on samples incubated respectively, for 0, 6, or 15 min at 4°C after heating and cooling cycles between 47°C and 4°C. These panels correspond to H4-0, H4-6, and H4-15 in Scheme 1. SCALTRD measurements were made at a scan rate of 5°C/min. Other details are presented under Experimental Procedures. Because of the finite spatial resolution of the x-ray films used in the streak film data measurements, the nonlamellar phases give rise to highly crowded, low-angle diffraction. The real space range covered by this low-angle scatter is represented as a cross-hatched band. Furthermore, in the interest of clarity the calculated lamellar repeat spacing *only* is included in the low-angle streak films where the L_{c0}, L_{c1}, L_{c2}, L_{β}, and L_{α} phases were encountered.

on the low- and wide-angle TRXRD and calorimetry. In the interests of clarity, only the calculated lamellar repeat spacings are shown in the low-angle region (top figure in each panel in Fig. 2). In the wide-angle region, all diffraction lines are shown (middle figure in each panel in Fig. 2). Cross-hatching is used to indicate the presence in the diffraction pattern of several unresolved reflections, as observed with certain of the nonlamellar phases (Fig. 2, *A1* and *B1*).

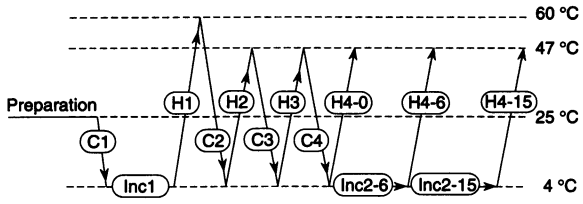

SCHEME 1. Thermal history protocols implemented in the study of the polymorphism and mesomorphism of dry monoelaidin and monoelaidin dispersed in excess water. Samples of dry monoelaidin were dispersed in water at ~25°C in the initial preparation step. The sample was then subjected to a first cooling step (C1) from 25°C to 4°C and immediately heated to 60°C in an initial heating step (H1). Inc1 refers to the fact that the sample, initially cooled to 4°C, was incubated at 4°C until synchrotron beam time became available (approximately 1 week) before subsequent heating. Inc2–6 and Inc2–15 refer, respectively, to a 6-min and a 15-min incubation at 4°C after the fourth cooling from 47°C. H4–0, H4–6, and H4–15 refer, respectively, to heating ramps from 4°C to 47°C after sample incubation for 0, 6, and 15 min at 4°C.

Behavior during initial heating scan (H1)

SCALTRD data collected during the initial heating scan (H1) are presented in Fig. 2 *A*. In the temperature range between 4°C and 38°C, a lamellar crystalline (L_{c0}) phase with a repeat spacing of 50.1 Å and 13 wide-angle reflections was observed (Table 1). At 38°C, the low-angle lamellar reflections broadened slightly and shifted to lower angles. At the same time, the sharp wide-angle reflections faded and gave way to a broad, diffuse band centered at ~4.5 Å (diffuse scatter is not shown in Fig. 2 *A2*). This new phase is of the L_{α} type and is characterized by a lamellar repeat spacing of ~51.0 Å. These structure changes were accompanied simultaneously by an endothermic transition observed by calorimetry, indicating that the phase transition at 38°C is of the L_{c0}-to-L_{α} type. The transition, which involves chain "melting" and imbibition of water, was completed at 51°C and 50°C by TRXRD and LSC, respectively, at a scan rate of 5°C/min. During the transition, a number of spatially unresolved reflections in the low-angle region (cross-hatched area in Fig. 2 *A1*) appeared at ~44°C and persisted up to 60°C. Earlier work involving temperature ramping TRXRD (see below) had shown that these reflections originate from the so-called X phase, which evolves from the lamellar and into the cubic (Im3m) phase upon heating (Caffrey, 1987, 1989). The X phase is characterized by multiple spotty reflections at very low angles. In the current study, we found that the temperature at which the X phase emerges during heating was not reproducible. Usually, however, it appeared in the vicinity of 38°C. (We note that when the sample succumbs to radiation damage, the X phase can be found at temperatures considerably below 38°C; unpublished data.) As was observed in the earlier work on hydrated monoelaidin, the X phase eventually converts to the Im3m cubic phase at higher temperatures. Because both X and Im3m have "crowded" low-angle diffraction patterns that overlap severely and because the spatial resolution of the x-ray

TABLE 1 X-ray diffraction data and phase designation for dry and hydrated monoelaidin at different temperatures and with different thermal histories

Hydration state	Thermal history*	T (°C)	Diffraction/scattering (Å)‡		Phase designation§
			Low-angle	Wide-angle	
Dry	H1	4	50.1 (10)	3.58W, 3.66S, 3.72M, 3.77M, 3.85VW, 3.92W, 3.99VW, 4.06W, 4.10VW, 4.20M, 4.25M, 4.30M, 4.35M, 4.40S	β
		51	50.1 (10)	3.79S, 3.84M, 3.93W, 4.08VW, 4.22W, 4.26M, 4.30M, 4.35M, 4.42S	β^{*}§§
		84	D28.0¶	D.45W	FI
Excess water	H1	4	50.1 (10)	3.58W, 3.66S, 3.72M, 3.77M, 3.85VW, 3.92W, 3.99VW, 4.06W, 4.20M, 4.26M, 4.31M, 4.36M, 4.42S	L_{c0}
		47	51.0 (2)	D4.5W	L_α, (X/Im3m)
		48	80–140‖	D4.5W	X/Im3m, (L_α)
	C2, C3, C4	45	51.0 (2)	D4.5W	L_α, (X/Im3m)
		45	70–125‖	D4.5W	X/Im3m, (L_α)
		10	61.0 (4)	4.28 VW,** 4.19S	L_β
	Inc2–15	4 (0)‡‡	60.5 (4)	4.07S	L_β
		4 (15)‡‡	50.1 (6)	3.43W, 3.61M, 3.77M, 3.82VW, 3.91VW, 4.02S, 4.07M, 4.18M	L_{c1}
	H2, H3, H4–0	4	60.0 (4)	4.05S	L_β
		47	50.0 (3)	D4.5W	L_α, (X/Im3m)
	H4–15	4	50.1 (6)	3.43W, 3.61M, 3.77M, 3.82VW, 3.91VW, 4.02S, 4.07M, 4.18M	L_{c1}
		20	62.3 (4)	4.1S	L_β, (L_{c1})
		33	50.1 (4)	3.61W, 3.75W, 3.90W, 4.00S, 4.10M, 4.19M, 4.42W	L_{c2}, (L_{c1})
		47	50.5 (2)	D4.5W	L_α, (X/Im3m)

*The notations used to indicate sample thermal history is taken from Scheme 1. H1 for dry monoelaidin indicates that this is an initial heating scan.
‡Except for the lamellar crystalline phases where the error is ± 0.1 Å, lamellar repeat values have an associated error of ±1 Å due to the difficulties in determining peak positions on very strong peaks and a low number of orders. Values are reported to one decimal place as a result of averaging over orders. Number of orders recorded are given in parentheses. The d-spacing of sharp wide-angle reflections are good to better than ± 0.1 Å.
§Coexisting phases are listed side by side separated by a comma. The minor phase/s is/are shown in parentheses.
¶D denotes that the peak was diffuse; all others are sharp. Intensity ratings are S, strong; M, medium; W, weak; and VW, very weak.
‖The d-spacing interval encompasses the reflections/scatter from the X/Im3m phase. The phases were designated as X and/or Im3m (X/Im3m) based on separate TRXRD measurements (data not shown) and previous work (Caffrey, 1987). The X-to-Im3m phase transition temperature was not determined.
**This reflection at 4.28 Å is seen on some but not all films.
‡‡Incubation time in minutes at 4°C is shown in the parentheses.
§§This phase is different from the β phase that was observed at 4°C for dry monoelaidin (see Discussion for details).

diffraction component of the SCALTRD measurement system is limited, it was not possible to identify the exact temperature of the X-to-Im3m transition in the current SCALTRD study. However, at the highest temperature accessed, namely 60°C, a recognizable Im3m diffraction pattern (three low-angle reflections in the ratio $1:\sqrt{2}:\sqrt{3}$) was obtained in these measurements. Thus, because of this ambiguity, we will refer to the transformation from the L_α to the X phase and to Im3m at high temperatures, simply as the L_α-to-X/Im3m transition. In the initial heating, this transition occurs at ~44°C. In all subsequent heating measurements the transition temperature is ~38°C. For the sake of clarity, the unresolved low-angle scattering associated with the X/Im3m phase region has been omitted from Fig. 2, *D1*, *E1*, and *F1*. The pronounced negative thermal expansion coefficient that characterizes this mixed-phase region (see Fig. 2 *A1*) under initial heating conditions persists in subsequent heating cycles (data not shown).

Cooling behavior (C2, C3, and C4)

A typical cooling measurement from 47°C to 4°C is shown in Fig. 2 *B* for a sample that had been heated previously to 55°C. At 47°C, the sample consists of coexisting L_α and Im3m phases, as evidenced by their characteristic low- and wide-angle diffraction patterns (Fig. 2, *B1* and *B2*). These two phases persist upon cooling down to 22°C. At 21°C, a new lamellar gel (L_β) phase emerges with a lamellar d-spacing of 62 Å and a single strong, sharp chain packing reflection at 4.19 Å in the wide-angle region. On occasion, the 4.19 Å reflection is accompanied by a weak reflection at 4.28 Å. The structure change seen by x-ray diffraction is apparent in the corresponding calorimetry measurement as an exotherm with an onset temperature of 22°C (Fig. 2 *B3*). The results obtained in the cooling mode were reproducible and independent of thermal history, provided the sample had been heated to at least 55°C. Failure to do so leaves a small and variable amount of the sample in the L_{c0} phase.

As a result, the subsequent cooling transition at 22°C is correspondingly less exothermic than observed when the sample starts out devoid of L_{c0}.

Isothermal behavior at 4°C (Inc2-15)

As noted above, we suspected that the L_β phase was metastable and that it would in time at low temperature transform to a more stable lamellar crystalline phase. This was tested by performing separate calorimetry and TRXRD measurements on a sample incubated at 4°C after the fourth cooling scan (C4 in Scheme 1). The results show that the sample starts out in the L_β phase (Fig. 2, *C1* and *C2*). With time, it transforms to a lamellar crystalline phase (L_{c1}) that has a wide-angle diffraction pattern distinct from that observed for the L_{c0} phase encountered during the initial heating measurements (Fig. 2, *A1* and *A2*). The lamellar repeat spacings of the L_β and L_{c1} phases were 60.6 Å and 50.1 Å, respectively, and were found to be independent of incubation time at 4°C on the time scale of the experiment (15 min, Fig. 2 *C1*). The calorimetric trace shows that the metastable L_β-to-L_{c1} isothermal transition is exothermic, as expected (Fig. 2 *C3*).

Fourth heating scans

The isothermal incubation at 4°C has been interrupted at three points in time to observe, by means of SCALTRD, the heating behavior of the sample that starts out in three different initial phases (Scheme 1). Thus, Fig. 2, *D*, *E*, and *F* show the fourth heating scan after 0 min (H4-0), 6 min (H4-6), and 15 min (H4-15) incubations at 4°C that correspond, respectively, to the sample before, during, and after the isothermal L_β-to-L_{c1} conversion described in Fig. 2 *C*. When the sample was heated immediately after the fourth cooling scan (H4-0), the L_β-to-L_α and L_α-to-X/Im3m transitions were seen at 23°C (Fig. 2 *D*) and 38°C (data not shown in Fig. 2 *D*), respectively. The fourth heating scan after a 15-min incubation at 4°C (H4-15) is shown in Fig. 2 *F*. In this condition, the calorimetric thermogram is complicated and is dominated by endotherms at ~13°C and 26°C and an exotherm at ~20°C. At low temperature, only the L_{c1} phase was apparent, as judged by TRXRD. (Occasionally, a single, very weak 001 lamellar reflection from the L_β phase was seen in this low temperature range after 15 min at 4°C.) Between 14°C and 25°C, the L_β phase that has the same low- and wide-angle diffraction behavior as the L_β phase seen in previous scans (Fig. 2, *B*, *C*, *D*, and *E*) made a transient appearance and coexisted with the L_{c1} phase. The former eventually transformed to a new lamellar crystalline phase, identified as L_{c2}, in a heat-releasing event at ~20°C (Fig. 2, *F1* and *F3*). The L_{c2} phase is different from the two other crystalline phases, L_{c0} and L_{c1}, reported above as judged by x-ray diffraction. The three lamellar crystalline phases will be discussed further below. Upon continued heating the L_α phase emerged at ~25°C, as evidenced by a series of lamellar reflections in the low-angle region (Fig. 2 *F1*) and a broad wide-angle band centered at ~4.5 Å. In the 25°C to 29°C range, the L_{c2} and L_α phases coexisted. Above 29°C, the L_α phase alone was present. At ~38°C, the X phase appeared, which developed into the Im3m phase at higher temperatures (data not shown in Fig. 2 *F*). Finally, at 47°C, the L_α phase and Im3m phase coexisted (data not shown).

After a 6-min incubation at 4°C, the sample included coexisting L_β and L_{c1} phases, as judged by TRXRD in the low temperature region (Fig. 2, *E1* and *E2*). Upon heating (H4-6), the thermogram showed endotherms at ~17°C, 23°C, and 26°C. An exothermic transition that is not obvious in the figure (Fig. 2 *E3*) was seen repeatedly at ~20°C. In both low- and wide-angle regions, the diffracted intensity associated with the L_β phase became stronger in the vicinity of 17°C at the expense of that from the L_{c1} phase. This suggests that the transition at 17°C during the fourth heating scan after a 6-min incubation at 4°C (H4-6) corresponds to the L_{c1}-to-L_β phase transition. From TRXRD, the L_β phase disappeared and converted to the L_{c2} phase, as evidenced by the wide-angle diffraction behavior and the presence of a small calorimetric exotherm at ~20°C. This conversion is completed at ~23°C, as judged by low- and wide-angle x-ray diffraction (Fig. 2, *E1* and *E2*). At 23°C, the L_β converts to the L_α phase, as judged by the emerging low-angle lamellar reflections and diffuse wide-angle scatter and the disappearing sharp reflection at 4.18 Å. During the L_β-to-L_α transition, the diffracted intensity from the L_β phase became weaker as that of the L_α phase grew stronger. In the L_β-to-L_α conversion range, the three phases, L_{c2}, L_β, and L_α, coexisted as judged by low- and wide-angle x-ray diffraction (Fig. 2, *F1* and *F2*). The L_β-to-L_α phase transition was completed at 26°C, above which the L_{c2} and L_α were found, as judged by calorimetry and x-ray diffraction. The L_{c2} phase began to transform to the L_α phase at ~26°C, as evidenced by calorimetry and wide-angle x-ray diffraction. Finally, the L_α-to-X/Im3m transition was seen at 38°C by low-angle x-ray diffraction. The X-to-Im3m transition, in the presence of the L_α phase, occurred at some unknown temperature between 38°C and 47°C and was completed below 47°C (data not shown). At 47°C, the L_α and Im3m phases coexisted.

Differential behavior upon heating and cooling

The temperature dependence of the lamellar and chain packing repeat spacings for the L_α and L_β phases recorded in the cooling (Fig. 2 *B1*) and heating (Fig. 2 *D1*) directions were the same. However, the corresponding temperature dependence and, indeed, the phase sequence involving the nonlamellar phases are sensitive to the direction of the temperature ramp. Thus, for example, the X phase evolves from the L_α phase at ~38°C and transforms into the Im3m phase with increasing temperature (as noted above the X-to-Im3m transition temperature was not determined in this study). The band of scattering intensity associated with the X and Im3m phases covers a range from 110 Å to 160 Å and 50 Å

to 100 Å at ~45°C at ~60°C, respectively (Fig. 2 *A1*). In contrast, the same scattering band associated with the Im3m phase, which extended from ~75 Å to 125 Å, did not change upon cooling from 47°C to 22°C. Moreover, the X phase did not appear upon cooling in the 47°C to 22°C range, as judged by small-angle x-ray diffraction.

Temperature ramping TRXRD

As noted previously, the temperature and spatial resolution associated with separate calorimetry and x-ray diffraction measurements is compromised somewhat in a SCALTRD study (Chung and Caffrey, 1992). Thus, separate TRXRD measurements were made to examine in detail the nature of the phases and their interconversions observed with monoelaidin upon temperature ramping at a scan rate of 4.7°C/min. Measurements were made using dry and hydrated monoelaidin. The results for the dry samples will be presented first. Streak film data collected during an initial heating scan for dry monoelaidin from 4°C to 90°C are included in Fig. 3 *A*. Calorimetry, performed separately, showed a single endotherm at ~57°C in this same temperature range (data not shown). At low temperatures below 57°C, the dry monoelaidin is in a lamellar crystalline phase, as evidenced by the evenly spaced reflections in the low-angle diffraction region and by a series of sharp, wide-angle reflections (Fig. 3 *A*). At 57°C, the sharp reflections in both wide- and low-angle regions begin to disappear and give way to corresponding diffuse scatter characteristic of the FI phase. Close inspection of the wide-angle diffraction lines in the 4°C to 57°C range shows a slight change at 3.66 Å (24.6°) and 3.85 Å (23.4°) in the vicinity of 45°C (Fig. 4). This suggests that the sample undergoes a polymorphic transition at this temperature. For reasons to be presented later, we will refer to this as the β-to-β^* transition. Interestingly, the change occurs without any alteration in the lamellar repeat, which remains fixed at 50.1 Å (Figs. 3 *A* and 4). Calorimetric measurements performed separately in the Mettler FP84, (data not shown) in the 4°C to 90°C range show a large endotherm at 57°C, which agrees with the TRXRD measurements reported above in support of a lamellar crystalline-to-FI transition at this temperature. However, no calorimetric evidence in support of the β-to-β^* polymorphic transition was obtained in these measurements.

The TRXRD result for the initial heating scan of monoelaidin dispersed in excess water is shown in Fig. 3 *B*. In the temperature range between 4°C and 45°C, the L_{c0} phase was observed. Upon heating, the L_{c0} phase transformed to the L_α phase at ~45°C. The 001 reflections from the L_{c0} (50.1 Å) and L_α (50.7 Å) phases were not resolved in the transition region. However, higher order lamellar reflections for each phase are clearly separated in the coexistence region. Upon continued heating up to 50°C, the L_α phase persists. This is in contrast to the results reported above under Simultaneous Calorimetry and TRXRD, where the L_α phase transforms to the X/Im3m at ~45°C. This result serves to highlight the variability of the results obtained, particularly under initial heating conditions.

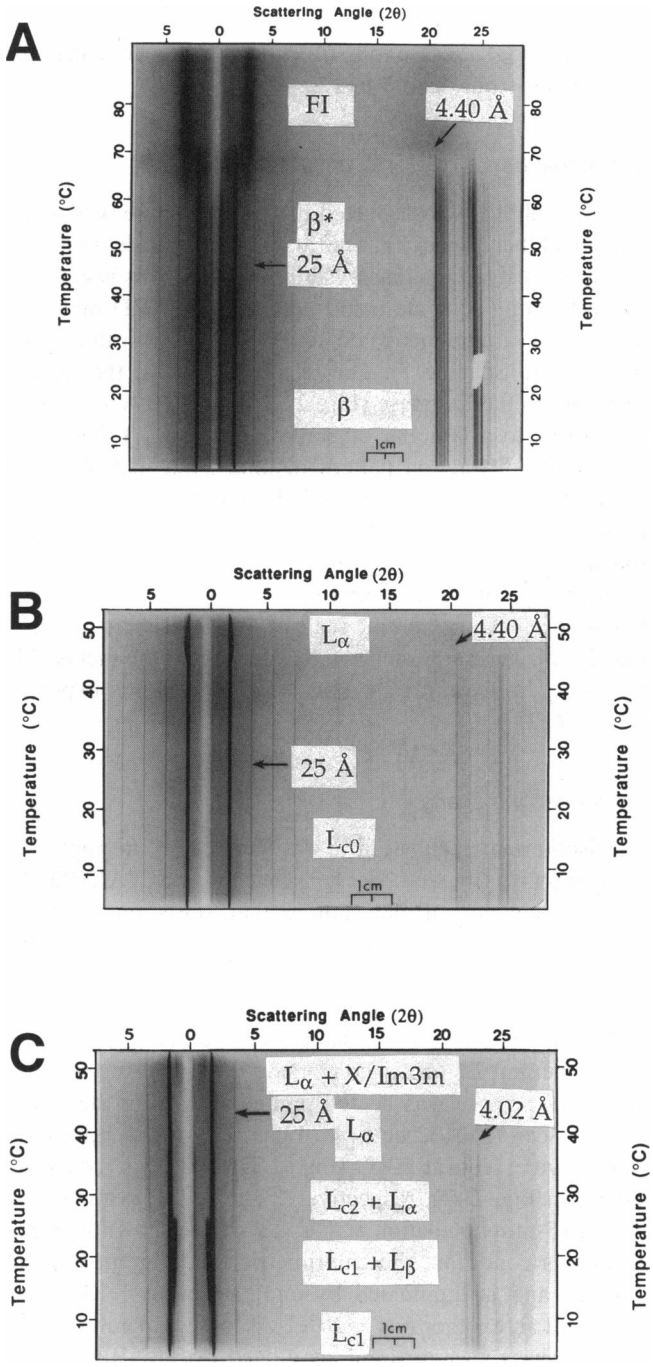

FIGURE 3 Streak film low- and wide-angle diffraction data on dry monoelaidin (*A*) and monoelaidin dispersed in excess water (*B, C*) recorded in the heating direction. The various polymorphs and mesophases as well as regions of phase coexistence are indicated. The heating rate was 4.7°C/min and the film was translated at a rate of 0.63 cm/min behind a 30-cm-long, 3-mm-wide slit. The clear strip at $2\theta = 0°$ marks the position of the beam stop.

The TRXRD results for the fourth heating scan on monoelaidin in excess water after a 15-min incubation at 4°C

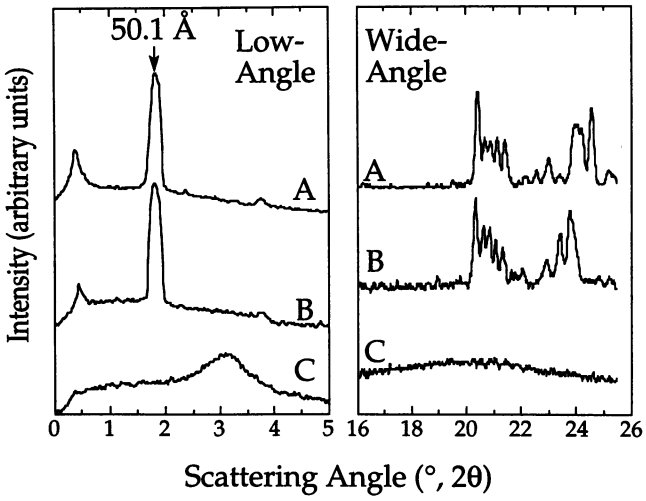

FIGURE 4 Low- and wide-angle diffraction from dry monoelaidin at (*A*) 4°C, (*B*) 51°C, and (*C*) 84°C recorded during the initial heating scan. The data were extracted from Fig. 3 *A* by using a 1D/2D soft laser scanning densitometer as described under Data Analysis.

(H4-15 in Scheme 1) are shown in Fig. 3 *C*. At temperatures below 12°C, the diffraction pattern is characteristic of the L_{c1} phase. At 12°C, the L_β phase emerges and coexists with the L_{c1} phase. The former has the same structural characteristics as the L_β phase seen in heating scans performed immediately after cooling (H4-0). Upon continued heating, the L_β phase begins to disappear at ~25°C and the low-angle reflections of the L_α phase emerge. Above 25°C, the diffraction pattern shows a characteristic lamellar crystalline phase (L_{c2}) in both low- and wide-angle regions. The L_{c2} phase coexisted with the L_α phase in the 25°C to 38°C range. In the 38°C to 48°C range, the L_α phase alone existed. At ~48°C, the X phase emerged and coexisted with the L_α for the duration of the temperature ramp.

The lamellar crystalline phases observed below (L_{c1}) and above (L_{c2}) the temperature range of L_β phase stability displayed the same low-angle but a different wide-angle diffraction behavior (Fig. 6). The d-spacings of reflections in the low- and wide-angle regions for the two phases are virtually identical. However, the intensity of diffracted peaks in the wide-angle region showed considerable differences. For example, reflections at 3.61 Å (25.0°) and 3.77 Å (23.9°) seen in the L_{C1} phase are almost invisible in the L_{c2} phase. Also, the relative intensities of the reflections at 4.02 Å (22.4°), 4.07 Å (22.1°), and 4.18 Å (20.5°) are different in the two phases.

Static x-ray diffraction

Comparing static diffraction patterns recorded on image plates at 25°C, we find that the L_{c0} phase observed with monoelaidin in excess water that had not been heat-treated is very similar to the β phase of dry monoelaidin. Specifically, the low-angle diffraction patterns for the two phases are identical (Fig. 7). The wide-angle diffraction patterns at 5°C are compared in Fig. 5. Generally, the d-spacings of the wide-angle reflections are similar for the two (Table 1, Fig. 5). The diffracted intensity distributions are also alike, although slight differences are registered at 3.77 Å (23.9°) and 4.40 Å (20.4°), both of which are stronger peaks in the β phase. Except for these minor disparities, the wide-angle diffraction of the two is virtually identical. The implication is that they are one and the same phase.

DISCUSSION

Dry monoelaidin

The dry, non-preheated lipid shows the β phase in a temperature range extending from 4°C to 45°C. At 45°C, the β phase transforms into the β^* phase, which eventually converts to the FI phase at 57°C. The two polymorphs, β and β^*, have an identical lamellar repeat spacing value of 50.1 Å but slightly different wide-angle diffraction behavior (Table 1, Fig. 4, *A* and *B*). Thermal expansion coefficients (α [= $1/d(\Delta d/\Delta T)$], where d is the repeat spacing and T is absolute temperature) for the lamellar and in-plane chain packing reflections are zero in the temperature range from 4°C to 45°C and 45°C to 65°C for the β and β^* phases, respectively.

Four crystalline polymorphs have been described for dry monoelaidin (Bailey, 1950; Carter and Malkin, 1947;

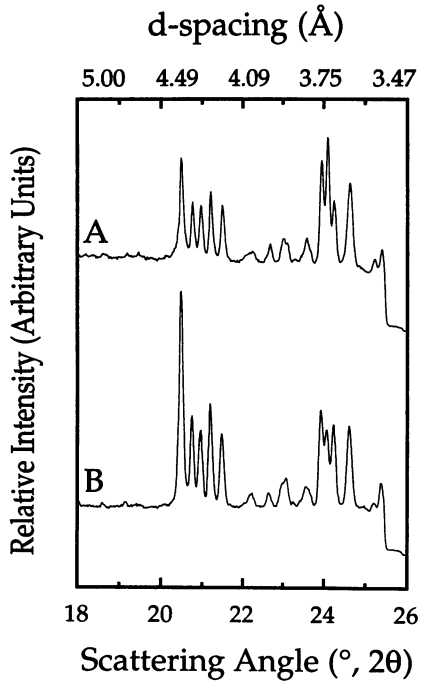

FIGURE 5 Wide-angle diffraction from the β phase (*A*) of dry monoelaidin and L_{c0} phase (*B*) of monoelaidin dispersed in excess water recorded on an image plate at 4°C. The diffracted intensities of each reflection for the L_{c0} and β phases were normalized by equalizing that of the peak at 3.66 Å (24.6°) in both cases. The data were processed as described under Experimental Procedures. The exposure times varied from 30 s to 1 min. The x-ray wavelength was 1.56 Å.

Maruyama et al., 1982). These include the sub-α (vitreous), α, β', and β (Carter and Malkin, 1947). Two of the polymorphs, β and β', are obtained by crystallization from solvents. The β' phase is obtained only by rapid crystallization from certain solvents, whereas the β phase is produced by slow crystallization (Bailey, 1950). When the melt (FI phase) is cooled, the α phase forms immediately. The α phase can convert reversibly to the sub-α phase upon further cooling (Bailey, 1950) (the α-to-sub-α transition temperature is not given in this reference). It can also transform spontaneously to the more stable β phase with time. In contrast to the latter, the β' polymorph can be obtained only by crystallization from solvents and is never a product of cooling from the melt.

The melting points of the sub-α (vitreous), α, β', and β phases are 29.5°C, 42°C, 56°C, and 58°C, respectively (Carter and Malkin, 1947). The d-spacings of the wide-angle x-ray reflections for the β' phase are 4.13 Å (strong; s), 3.88 Å (weak; w), 3.73 Å (w), and 3.59 Å (w) and for the β phase, 4.55 Å (s), 4.38 Å (w), 4.14 Å (w), and 3.93 Å (s). The wide-angle diffraction behavior of the sub-α and α phases of monoelaidin has not been reported. For the related monoacylglycerols, monopalmitin and monostearin, the corresponding wide-angle reflections are observed at 4.7 Å (w), 4.2 Å (very strong; vs), and 3.8 Å (w) for the α phase and 4.1 Å (vs), 3.9 Å (medium; m), 3.7 Å (m), and 3.6 Å (m) for the sub-α phase (Lutton and Jackson, 1948).

The final step taken by the vendor (Nu Chek Prep) before bottling monoelaidin for distribution is to melt the lipid. Because the β' phase can only be obtained by crystallization from solvents, it is excluded from the range of possible phases that exist in dry solid monoelaidin upon shipment. Furthermore, because the "as received" monoelaidin has a melting temperature of 57°C as determined by HSDSC, these data together suggest that the melting transition observed in this study is of the β-to-FI type. X-ray diffraction measurements eliminate the possibility that the starting phase is of the sub-α or α type because the strongest wide-angle reflection in each case is observed at 4.2 Å (Lutton and Jackson, 1948). The d-spacings of the wide-angle x-ray reflections recorded in the dry monoelaidin below the melting point in this study (Table 1) agree qualitatively with those reported by Carter and Malkin for the β phase (Carter and Malkin, 1947). Quantitative differences might be ascribable to disparities in such experimental factors as sample-to-film distance determination and x-ray wavelength calibration (Carter and Malkin used $\lambda = 1.5386$ Å for Cu Kα; we used 1.542 Å).

Monoelaidin/water

Behavior during initial heating (H1)

The L_{c0} phase is found in nonpreheated monoelaidin/water samples in the temperature range extending from 4°C to 38°C. While preparing such samples for calorimetry and SCALTRD, we noticed that the dry lipid does not imbibe water in the vicinity of room temperature (20–30°C). Thus, for example, when water is placed in contact with the dry monoelaidin powder, it remains as a beaded-up droplet with no visible interaction taking place. In contrast, the appearance of the mechanically mixed sample is distinctly different from that made simply by bringing the lipid and water into direct contact. However, the two samples have identical phase behavior, as evidenced by x-ray diffraction and calorimetry. Based on this observation, we speculated that in the absence of heating, the dry lipid, originally in the so-called β phase, when dispersed in water simply coexists with water. Under Results above, we have referred to the lamellar crystalline phase adopted by nonpreheated, dry monoelaidin dispersed in excess water as the L_{c0} phase. Comparison of the low- and wide-angle diffraction patterns for the L_{c0} and β phases shows clearly that the two represent one and the same phase or polymorph (Table 1, compare Figs. 5, *A* and *B*, and 7). The slightly different intensities associated with some of the reflections in the two phases can arise by a small differential orientation of crystallites in the two preparations.

When first heated, the L_{c0} phase transforms to the L_α phase at 38°C. Coexistence of the two phases during the transition indicates that the L_{c0}-to-L_α phase change is two-state without the appearance of intermediates to within the sensitivity limits of the detector (Fig. 3 *B*). With continued heating, the L_α converts to the so-called X phase (Caffrey, 1987, 1989) at ~45°C. The latter is characterized by a "crowded" and spotty diffraction pattern at very low angles. As mentioned earlier, the L_α-to-X transition temperature is not reproducible. Regardless of the care taken to reproduce sample preparation and thermal pretreatment conditions, the onset of the L_α-to-X transition was found to occur anywhere in the ~38°C to 45°C range. With further heating, the X phase transforms to the Im3m phase. Unfortunately, the temperature of this transition could not be determined under current experimental conditions because of the low spatial resolution available in the x-ray diffraction measurements. This aspect of hydrated monoelaidin mesophase behavior was not examined further in this study.

Cooling behavior (C2, C3, and C4)

Hydrated monoelaidin samples that had been preheated previously to 55°C exhibit Im3m/L_α phase coexistence in the 47°C to 22°C range upon cooling. The L_α and the metastable Im3m phase transform simultaneously to the L_β phase at 22°C, as judged by TRXRD (Fig. 2, *B2* and *B3*). Upon further cooling, the L_β phase existed in the range from 22°C to 4°C. The calorimetric trace recorded from 47°C to 4°C shows a single exotherm at 22°C. Identical cooling calorimetric and TRXRD scans from 47°C to 4°C were obtained regardless of the previous thermal history of the sample (Fig. 2 *B*), provided the sample had been heated to at least 55°C. The range of d-spacings associated with the low-angle reflections from the Im3m phase remains constant with temperature in this range. In contrast, in the

heating direction, the corresponding d-spacing values decrease dramatically with temperature from 70 Å to 125 Å at 45°C and from 50 Å to 100 Å at 60°C (Fig. 2 *A*). The decrease in the lattice parameter with increasing temperature can arise because water is released to the bulk and/or the lipid bilayer thickness decreases at higher temperature. According to Lutton's temperature-composition phase diagram for the monoelaidin/water system (Lutton, 1965), the cubic-to-(cubic + excess water) phase boundary shifts in the direction of a less hydrated lipid as temperature increases. Therefore, a loss of water from the cubic matrix at higher temperatures is expected, and this alone should effect a decrease in the lattice parameter. In the cooling direction, presumably bulk water must access the deepest labyrinths of the cubic mesophase to allow the unit cell to swell if the behavior of the system is to follow that seen under equilibrium conditions (Lutton, 1965). The fact that the lattice parameter remains constant during a cooling scan performed at a rate of −5°C/min suggests that water uptake does not occur on this time scale. As a result, the relatively rapidly cooled cubic phase has a water deficit when compared to the hydration level of this same cubic phase under equilibrium conditions. This suggests that the particular cubic phase accessed in the cooling direction in the current study is structurally metastable with respect to the more fully hydrated equilibrated version of same.

Behavior upon heating immediately after cooling (H2, H3, and H4-0)

Immediate heating SCALTRD after cooling to 4°C showed the L_β-to-L_α phase transition occurring at 23°C (Fig. 2 *D*). The L_α-to-X/Im3m phase transition was seen at ~38°C. Calorimetric measurements show a single endotherm at ~23°C corresponding to the L_β-to-L_α transition. The lamellar repeat and wide-angle d-spacing are 51.0 Å and 4.5 Å for the L_α phase at 47°C. The corresponding values for the L_β phase are 60.0 Å and 4.05 Å, respectively, at 4°C. The thermal expansion coefficient, α, for the lamellar repeat and chain packing reflection of the L_β phase are 0.005 and 0.0006 K^{-1} in the temperature range from 4°C to 22°C, indicating that the unit cell size of the L_β phase increases with temperature. The corresponding α value for the lamellar repeat of the L_α phase was -0.001 K^{-1} in the temperature range from 23°C to 47°C. The α value of the L_α phase for chain packing was not determined.

Isothermal behavior at 4°C (Inc2-15)

Immediately upon cooling of fully hydrated monoelaidin from 47°C to 4°C, a metastable form of the L_β emerges. Within 6 min of incubation at 4°C, the latter converts spontaneously and isothermally to the L_{c1} phase (Fig. 2 *C*). The d-spacings of both the L_β and L_{c1} phases in the low- and wide-angle regions of the diffraction pattern remain constant during the course of the 4°C incubation. The TRXRD data show that the L_β and L_{c1} phases alone coexist during the transition, suggesting that the transition is two-state without the appearance of intermediates to within the sensitivity limits of the x-ray detector. The exotherm associated with the L_β-to-L_{c1} phase transition was detected by calorimetry (Fig. 2 *C3*).

Fourth heating scan after 15-min incubation at 4°C (H4-15)

The L_{c1} phase alone and occasionally with a trace of the L_β phase existed after more than an 8-min incubation at 4°C upon cooling from 47°C (Fig. 2 *F*). When the sample was subsequently heated to ~15°C, a portion of the L_{c1} phase transformed to the higher energy L_β phase. The endotherm observed by LSC at 15°C with a ΔH value of 0.7 kcal/mol is associated with this transition (Fig. 1 *B4*). The isothermal L_β-to-L_{c1} transition has an associated ΔH of 9.0 kcal/mol (Fig. 2 *C*). This suggests therefore that approximately one-tenth of the lipid goes through the L_{c1}-to-L_β transition at 15°C under these conditions. The newly formed L_β phase subsequently transformed to the L_{c2} phase at ~20°C in a heat-releasing event, as evidenced the accompanying exotherm (ΔH = −0.7 kcal/mol, Fig. 1, *A5* and *B4*). Wide-angle diffraction analysis shows that the L_{c2} and L_{c1} phases are distinct and represent different polymorphs (compare Fig. 6, *A* and *C*). Evidence for a direct L_{c1}-to-L_{c2} transition has not been found. We speculate that the L_β phase formed from the L_{c1} phase upon heating is metastable with respect to the L_{c2} phase. The L_{c2} and L_{c1} polymorphs are close in energy and do not interconvert on the time scale and under the conditions of these experiments. With continued heating, the residual L_{c1} phase (~92% of the lipid), which had not transformed into the L_β phase, converts to the L_α phase

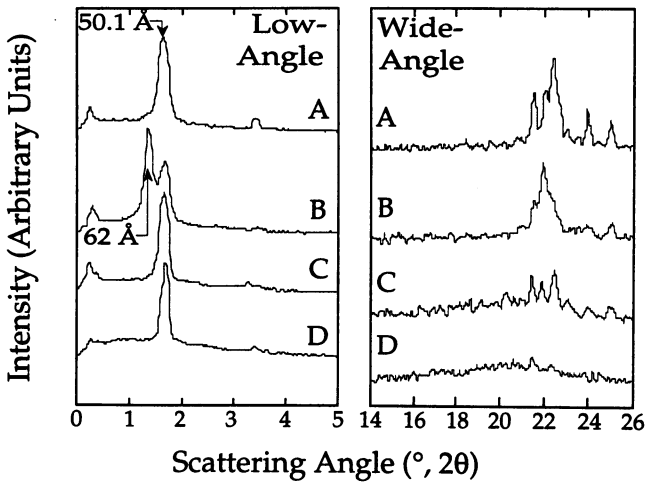

FIGURE 6 Low- and wide-angle x-ray diffraction from the L_{c1} (*A*), L_{c1} + L_β (*B*), L_{c2} + L_α (*C*), and L_α (*D*) phases of monoelaidin dispersed in excess water during a fourth heating scan after a 15-min incubation at 4°C (H4-15 in Scheme 1). The data were extracted from Fig. 3 *C* by using a 1D/2D soft laser scanning densitometer as described under Data Analysis at 4.9°C (*A*), 21.5°C (*B*), 32.9°C (*C*), and 44.9°C (*D*). The wide-angle data have been smoothed by computing moving averages (window size = 9 data points).

at 26°C. At essentially the same temperature, the L_{c2}-to-L_α phase transition takes place. Because of the limited temperature and spatial resolution of the TRXRD measurements, it was not possible to resolve the L_{c1}-to-L_α and L_{c2}-to-L_α transitions. Calorimetry shows a broad and asymmetric transition at 26°C (Fig. 1, *A5* and *B4*), which likely encompasses both transitions.

Description of phase behavior

The polymorphism, mesomorphism, and metastable behavior of monoelaidin in excess water in the 4°C and 60°C range are shown schematically in Scheme 2. Then dry monoelaidin in the L_{c0} phase is dispersed in excess water at room temperature, and it does not imbibe water provided it is not heated above 38°C. Thus, it remains in the same polymorphic form as the dry lipid identified as the β phase in the glyceride literature (Bailey, 1950; Carter and Malkin, 1947). With increasing temperature, the L_{c0} phase converts to the L_α phase at 38°C in a heat-absorbing step (ΔH = 7.3 kcal/mol). With continued heating, the X phase appears and gives way to the Im3m phase at higher temperatures. The temperature of the L_α-to-X/Im3m transition was not shown to be reproducible in this study. However, in the heating direction, the X-to-Im3m transition was found to be completed at 47°C, above which the L_α and Im3m phases coexist. Thus, the latter corresponds to the (L_α + X)-to-(L_α + Im3m) transition. When cooled from 47°C, the coexisting L_α and Im3m phases convert via an exothermic

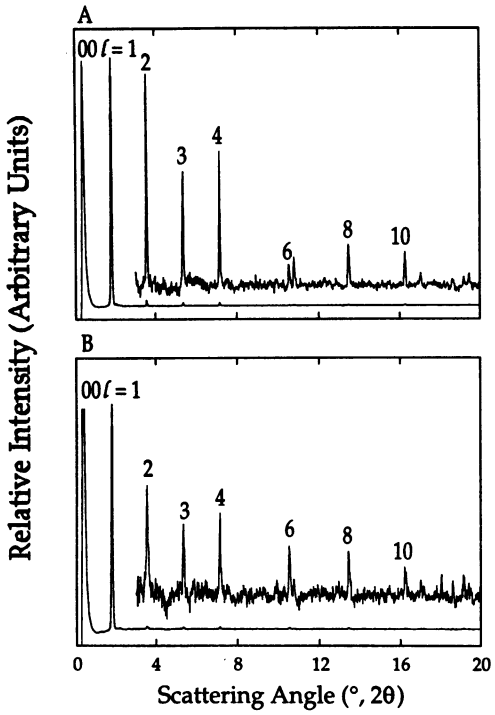

FIGURE 7 I-2θ diffracted intensity profiles of dry monoelaidin (*A*) and non-preheated monoelaidin in excess water (*B*) at 4°C. The lamellar repeat order number is indicated above each peak. The lamellar repeat spacing was 50.1 Å. We note that the peak on the high angle side of the 006 reflection at 11.3° does not index as a lamellar reflection and most likely arises from in-plane diffraction.

SCHEME 2. Schematic representation of the various polymorphs and liquid crystalline phases accessed by dry monoelaidin and monoelaidin dispersed in excess water in the 4°C to 60°C range. Transition temperatures indicated to the left or right of solid vertical arrows correspond to onset temperatures. Associated enthalpy changes are indicated below the transition temperatures in units of kcal/mol. Wavy arrows correspond to isothermal transitions at the temperature indicated. Dashed arrows indicate that only a fraction of the sample undergoes the particular transition. The positions along the vertical axis of the horizontal dashed and solid lines correspond, respectively, to the relative energy levels of the metastable and equilibrium phases or polymorphs.

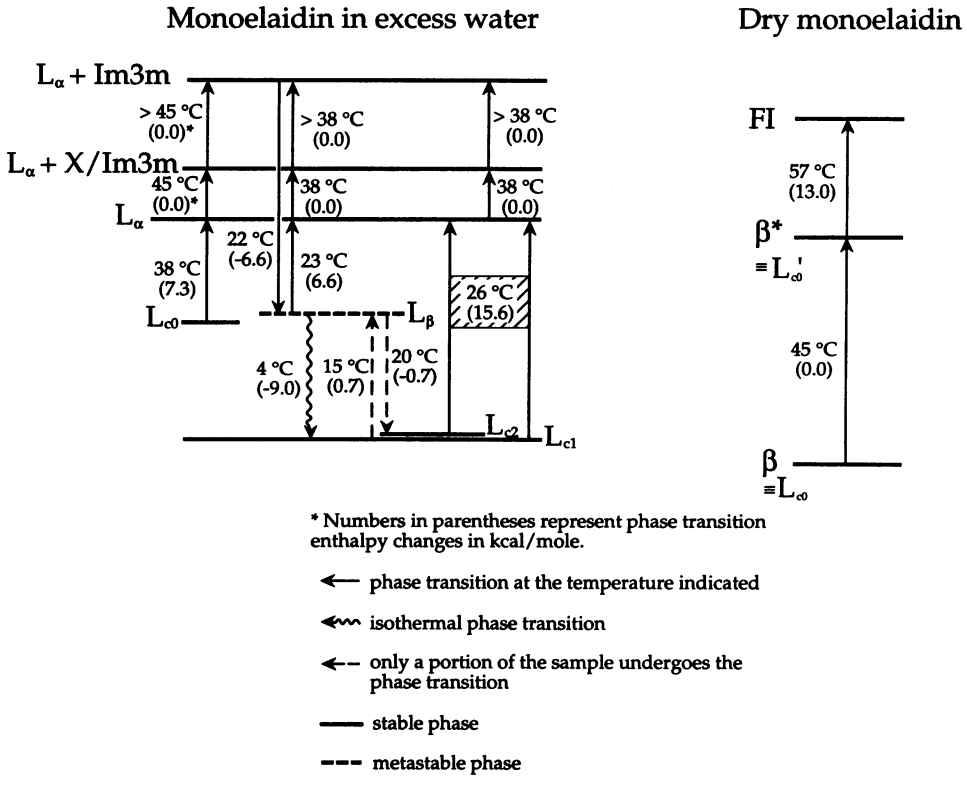

transition ($\Delta H = -6.6$ kcal/mol) to a metastable L_β phase at 22°C, which persists down to 4°C. If the sample is heated immediately after being cooled to 4°C, the L_β-to-L_α transition is observed at 23°C ($\Delta H = 6.6$ kcal/mol). On the other hand, if the sample that was cooled initially to 4°C is held at this temperature, it converts isothermally from the metastable L_β phase to the L_{c1} phase in ~8 min ($\Delta H = 9.0$ kcal/mol). When heated from 4°C at the rate of 5°C/min, a portion of the sample in the L_{c1} phase converts to the L_β phase at 15°C. The ΔH value for this transition (0.7 kcal/mol) indicates that ~10% of the lipid undergoes the L_{c1}-to-L_β phase transition. The L_β is again metastable at 20°C and transforms to the L_{c2} phase at this temperature. At this point in thermal treatment, the sample consists of the L_{c1} and L_{c2} phases. Upon continued heating, both crystalline polymorphs transform to the L_α phase in a relatively broad endothermic transition, which begins at ~26°C. We were not able to identify separate L_{c1}-to-L_α and L_{c2}-to-L_α transitions in the course of these measurements. Furthermore, we found no evidence for an L_{c1}-to-L_{c2} interconversion under present experimental conditions.

CONCLUSIONS

It is clear from this study that the polymorphic and mesomorphic behavior of monoelaidin dispersed in excess water is quite complex. Complications arise because of a rich polymorphism exhibited in the low temperature region where at least three distinct but structurally similar lamellar crystalline polymorphs have been identified and four liquid crystalline phases have been found at higher temperatures. Several of the polymorphs and mesophases encountered are metastable and transform to more stable states isothermally and/or in the course of thermal cycling. Despite the complexities, the individual polymorphs and mesophases have been identified and structurally characterized and their respective thermodynamic stabilities established based on a combination of x-ray diffraction and calorimetric measurements performed separately and simultaneously. Because this system exhibits a profound thermal history-dependent behavior, the daunting task of establishing the relationships in time and temperature between the various polymorphs and mesomorphs was made possible by implementing the SCALTRD method. It is in this type of study where complexities abound that the SCALTRD technique proves its worth. In the current investigation, the SCALTRD measurements were synchrotron radiation based. A SCALTRD apparatus is now being built that will operate on a conventional x-ray source, which should make the method that much more accessible. We note that thermal history-dependent behavior is not unique to the hydrated neutral lipids but is quite a general phenomenon seen in materials as disparate as complex polymers and simple inorganic compounds.

We thank the entire CHESS (National Science Foundation grant DMR 12822) and MacCHESS (National Institutes of Health grant RR-014646) staff for their invaluable help and support. We are grateful to J. L. Hogan, A. Mencke, J. Briggs, A-C. Cheng for valuable discussions and for their help at the synchrotron. We also thank S. Kirchner, R. Koynova, J. Wang for comments on the manuscript.

This work was supported by a grant from the National Institutes of Health (DK36849 and DK 45295) and the National Science Foundation (DIR 9016683).

REFERENCES

Bailey, A. E. 1950. Melting and Solidification of Fats. Interscience Publishers, New York.

Briggs, J., and M. Caffrey. 1994. The temperature-composition phase diagram of monomyristolein in water: equilibrium and metastability aspects. *Biophys. J.* 66:573–587.

Caffrey, M. 1984. X-Radiation damage of hydrated lecithin membranes detected by real-time X-ray diffraction using wiggler enhanced synchrotron radiation as the ionizing radiation source. *Nucl. Instr. Methods.* 222:329–338.

Caffrey, M. 1985. Kinetics and mechanism of the lamellar gel/lamellar liquid crystal and lamellar/inverted hexagonal phase transitions in phosphatidylethanolamine: a real-time x-ray diffraction study using synchrotron radiation. *Biochemistry.* 24:4826–4844.

Caffrey, M. 1987. Kinetics and mechanism of transitions involving the lamellar, cubic, inverted hexagonal, and fluid isotropic phases of hydrated monoalylglycerides monitored by time-resolved x-ray diffraction. *Biochemistry.* 26:6349–6363.

Caffrey, M. 1989. A lyotropic gradient method for liquid crystal temperature-composition-mesomorph diagram construction using time-resolved x-ray diffraction. *Biophys. J.* 55:47–52.

Carter, M. G. R., and T. Malkin. 1947. An x-ray and thermal examination of the glycerides. Part VIII. Glycerides of erucic, brassidic, oleic, and elaidic acids. *J. Chem. Soc.* 554–558.

Cheng, A.-c., J. L. Hogan, and M. Caffrey. 1993. X-rays destroy the lamellar structure of model membranes. *J. Mol. Biol.* 229:291–294.

Chung, H., and M. Caffrey. 1992. Direct correlation of structure changes and thermal events in hydrated lipid established by simultaneous calorimetry and time-resolved x-ray diffraction. *Biophys. J.* 63:438–447.

Garti, N., and K. Sato. 1988. Crystallization and Polymorphism of Fats and Fatty Acids. Marcel Dekker, New York. 450 pp.

Kekicheff, P., C. Grabielle-Madelmont, and M. Ollivon. 1989. Phase diagram of sodium dodecylsulfate-water system. 1. A calorimetric study. *J. Colloid Int. Sci.* 131:112–132.

Lutton, E. S. 1965. Phase behavior of aqueous systems of monoglycerides. *J. Am. Oil Chem. Soc.* 42:1068–1070.

Lutton, E. S., and Jackson, F. L. 1948. The polymorphism of 1-monostearin and 1-monopalmitin. *J. Am. Chem. Soc.* 70:2445–2449.

Mariani, P., V. Luzzati, and H. Delacroix. 1988. Cubic phases of lipid-containing systems. Structure analysis and biological implications. *J. Mol. Biol.* 204:165–189.

Martin, J. 1953. Preparation of saturated and unsaturated symmetrical monoglycerides. *J. Am. Chem. Soc.* 75:5482–5486.

Maruyama, T., I. Niiya, M. Okada, and T. Matsumoto. 1982. Studies on polymorphism of monoglyceride. XI. Transitions of crystal modification of trans-monounsaturated monoglycerides. *J. Oil Chem. Soc. Jpn.* 31: 218–221.

McIntosh, T. J., A. D. Magid, and S. A. Simon. 1989. Repulsive interactions between unchanged bilayers. Hydration and fluctuation pressures for monoacylglycerides. *Biophys. J.* 55:897–904.

Small, D. M. 1986. The Physical Chemistry of Lipids. Handbook of Lipid Research. Plenum Press, New York. 672 pp.